Strong magnetic response of submicron Silicon particles in the infrared

A. García-Etxarri,[1] R. Gómez-Medina,[2] L. S. Froufe-Pérez,[2] C. López,[2] L. Chantada,[3] F. Scheffold,[3] J. Aizpurua,[1] M. Nieto-Vesperinas,[2] and J. J. Sáenz[1,4,*]

[1]*Centro de Fisica de Materiales CSIC-UPV/EHU and Donostia International Physics Center (DIPC), Paseo Manuel Lardizabal 4, 20018 Donostia-San Sebastian, Spain*
[2]*Instituto de Ciencia de Materiales de Madrid, CSIC, Campus de Cantoblanco, 28049 Madrid, Spain*
[3]*Department of Physics, University of Fribourg, Chemin du Muse 3, 1700 Fribourg, Switzerland*
[4]*Departamento de Física de la Materia Condensada and Instituto "Nicolás Cabrera," Universidad Autónoma de Madrid, 28049 Madrid, Spain*
[*]*juanjo.saenz@uam.es*

Abstract: High-permittivity dielectric particles with resonant magnetic properties are being explored as constitutive elements of new metamaterials and devices. Magnetic properties of low-loss dielectric nanoparticles in the visible or infrared are not expected due to intrinsic low refractive index of optical media in these regimes. Here we analyze the dipolar electric and magnetic response of lossless dielectric spheres made of moderate permittivity materials. For low material refractive index ($\lesssim 3$) there are no sharp resonances due to strong overlapping between different multipole contributions. However, we find that Silicon particles with index of refraction ~ 3.5 and radius ~ 200nm present strong electric and magnetic dipolar resonances in telecom and near-infrared frequencies, (i.e. at wavelengths $\approx 1.2 - 2\mu$m) without spectral overlap with quadrupolar and higher order resonances. The light scattered by these Si particles can then be perfectly described by dipolar electric and magnetic fields.

OCIS codes: (290.5850) Scattering, particles; (160.1190) Anisotropic optical materials; (160.3820) Magneto-optical materials.

References and links

1. H. C. van de Hulst, *Light Scattering by Small Particles* (Dover, 1981).
2. C. F. Bohren and D. R. Huffman, *Absorption and Scattering of Light by Small Particles* (John Wiley &Sons, 1998).
3. M. I. Mishchenko, L. D. Travis, and A. A. Lacis, *Scattering, Absorption, and Emission of Light by Small Particles* (Cambridge Univ. Press, 2002).
4. L. Novotny and B. Hecht, *Principles of Nano-Optics*, (Cambridge Univ. Press, 2006).
5. E. M. Purcell and C. R. Pennypacker, "Scattering and absorption of light by nonspherical dielectric grains," Astrophys. J. **186**, 705–714 (1973).
6. B. T. Draine, "The discrete dipole approximation and its application to interstellar graphite grains," Astrophys. J. **333**, 848–872 (1988).
7. W. L. Barnes, A. Dereux, and T. W. Ebbesen, "Surface plasmon subwavelength optics," Nature **424**, 824–830 (2003).
8. N. Engheta and R.W. Ziolkowski, "A positive future for double-negative metamaterials," IEEE Trans. Microwave Theory Tech. **53**, 1535–1556 (2005).

#137123 - $15.00 USD Received 25 Oct 2010; revised 23 Dec 2010; accepted 15 Feb 2011; published 28 Feb 2011

9. J. B. Pendry, "Beyond metamaterials," Nature Mater. **5**, 763–764 (2006).
10. V. M. Shalaev, "Optical negative-index metamaterials," Nat. Photonics **1**, 41–48 (2007).
11. P. J. Schuck, D. P. Fromm, A. Sundaramurthy, G. S. Kino, and W. E. Moerner, "Improving the mismatch between light and nanoscale objects with gold bowtie nanoantennas," Phys. Rev. Lett. **94**, 017402 (2005).
12. F. Neubrech, A. Pucci, T. W. Cornelius, S. Karim, A. Garca-Etxarri, and J. Aizpurua, "Resonant plasmonic and vibrational coupling in a tailored nanoantenna for infrared detection," Phys. Rev. Lett. **101**, 157403 (2008).
13. T. H. Taminiau, F. D. Stefani, F. B. Segerink, and N. F. Van Hulst, "Optical antennas direct single-molecule emission," Nat. Photonics **2**, 234-237 (2008).
14. A. Alù and N. Engheta, "The quest for magnetic plasmons at optical frequencies," Opt. Express **17**, 5723–5730 (2009).
15. A. Alú, and N. Engheta, "Dynamical theory of artificial optical magnetism produced by rings of plasmonic nanoparticles," Phys. Rev. B **78**, 085112 (2008).
16. K. C. Huang, M. L. Povinelli, and J. D. Joannopoulos, "Negative effective permeability in polaritonic photonic crystals," Appl. Phys. Lett. **85**, 543–545 (2004).
17. C. L. Holloway, E. F. Kuester, J. Baker-Jarvis, and P. Kabos, "A double-negative (DNG) composite medium composed of magnetodielectric sphercal particles embedded in a matrix," IEEE Trans. Antennas Propag. **51**, 2596–2603 (2003).
18. M. S. Wheeler, J. S. Aitchison, and M. Mojahedi, "Three-dimensional array of dielectric spheres with an isotropic negative permeability at infrared frequencies," Phys. Rev. B **72**, 193103 (2005).
19. V. Yannopapas and A. Moroz, "Negative refractive index metamaterials from inherently non-magnetic materials for deep infrared to terahertz frequency ranges," J. Phys.: Condens. Matter **17**, 3717–3734 (2005).
20. A. Ahmadi and H. Mosallaei, "Physical configuration and performance modelling of all-dielectric metamaterials," Phys. Rev. B **77**, 045104 (2008).
21. M. S. Wheeler, J. S. Aitchison, J. I. L. Chen, G.A. Ozin, and M. Mojahedi, "Infrared magnetic response in a random silicon carbide micropowder," Phys. Rev. B **79**, 073103 (2009).
22. L. Jyhlä, I. Kolmakov, S. Maslovski, and S. Tretyakov, "Modeling of isotropic backward-wave materials composed of resonant spheres," J. Appl. Phys. **99**, 043102 (2006).
23. L. Peng, L. Ran, H. Chen, H. Zhang, J. A. Kong, and T. M. Grzegorczyk, "Experimental observation of left-handed behavior in an array of standard dielectric resonators," Phys. Rev. Lett. **98**, 157403 (2007).
24. J. A. Schuller, R. Zia, T. Taubner, and M. L. Brongersma, "Dielectric metamaterials based on electric and magnetic resonances of silicon carbide particles," Phys. Rev. Lett. **99**, 107401 (2007).
25. K. Vynck, D. Felbacq, E. Centeno, A. I. Cabuz, D. Cassagne, and B. Guizal, "All-dielectric rod-type metamaterials at optical frequencies," Phys. Rev. Lett. **102**, 133901 (2009).
26. M. Notomi, "Theory of light propagation in strongly modulated photonic crystals: refractionlike behavior in the vicinity of the photonic band gap," Phys. Rev. B **62**, 10696–10705 (2000).
27. S. Foteinopoulou and C. M. Soukoulis, "Negative refraction and left-handed behavior in two-dimensional photonic crystals," Phys. Rev. B **67**, 235107 (2000).
28. R. K. Mongia and P. Bhartia, "Dielectric resonator antennas-A review and general design relations for resonant frequency and bandwidth," Int. J. Microwave Millimeter-Wave Comput.-Aided Eng. **4**, 230-247 (1994).
29. R. C. J. Hsu, A. Ayazi, B. Houshmand, and B. Jalali, "All-dielectric photonic-assisted radio front-end technology," Nat. Photonics **1**, 535-538 (2007).
30. J. A. Schuller and M. L. Brongersma, "General properties of dielectric optical antennas," Opt. Express **17**, 24084–24095 (2009).
31. M. M. Sigalas, D. A. Fattal, R. S. Williams, S.Y. Wang, and R. G. Beausoleil, " Electric field enhancement between two Si microdisks," Opt. Express **15**, 14711–14716 (2007).
32. Q. Zhao, J. Zhou1, F. Zhang, and D. Lippens, "Mie resonance-based dielectric metamaterials," Mater. Today **12**, 60–69 (2009).
33. P. Chylek, J. T. Kiehl and M. K. W. Ko, "Optical levitation and partial-wave resonances," Phys. Rev. A **18**, 2229–2233 (1978)
34. G. Videen and W. S. Bickel, "Light-scattering resonances in small spheres," Phys. Rev. A **45**, 6008–6012 (1992).
35. E.D.Palik, *Handbook of Optical Constants of Solids* (Academic Press, 1985).
36. S. Albaladejo, R. Gómez-Medina, L. S. Froufe-Pérez, H. Marinchio, R. Carminati, J. F. Torrado, G. Armelles, A. García-Martín, and J. J. Sáenz, "Radiative corrections to the polarizability tensor of an electrically small anisotropic dielectric particle," Opt. Express **18**, 3556–3567 (2010).
37. M. Nieto-Vesperinas, J. J. Sáenz, R. Gómez-Medina, and L. Chantada, "Optical forces on small magnetodielectric magnetic particles," Opt. Express **18**, 11428–11443 (2010).
38. M. Born and E. Wolf, *Principles of Optics*, 7th ed. (Cambridge Univ. Press, 1999), Sec. 2.3.
39. O. N. Singh and A. Lakhtakia, eds. *Electromagnetic Fields in Unconventional Materials and Structures* (Wiley, 2000).
40. L. Tsang and J. A. Kong, *Scattering of Electromagnetic Waves-Advanced Topics* (Wiley, 2001).
41. R. Carminati and J. J. Sáenz, "Density of states and extinction mean free path of waves in random media: dispersion relations and sum rules," Phys. Rev. Lett. **102**, 093902 (2009).

#137123 - $15.00 USD Received 25 Oct 2010; revised 23 Dec 2010; accepted 15 Feb 2011; published 28 Feb 2011

42. P. D. García, R. Sapienza, A. Blanco, and C. López, "Photonic glass: a novel random material for light," Adv. Mater. **19**, 2597–2602 (2007).
43. M. Reufer, L. F. Rojas-Ochoa, S. Eiden, J. J. Sáenz, and F. Scheffold, "Transport of light in amorphous photonic materials," Appl. Phys. Lett. **91**, 171904 (2007).
44. M. Ibisate, D. Golmayo, and C. López, "Photonic crystals: silicon direct opals," Adv. Mater. **28**, 2899–2902 (2009).
45. S. Albaladejo, M. I. Marqués, M. Laroche and J. J. Sáenz, "Scattering forces from the curl of the spin angular momentum of a light field," Phys. Rev. Lett. **102**, 113602 (2009).
46. P. C. Chaumet and A. Rahmani, "Electromagnetic force and torque on magnetic and negative-index scatterers," Opt. Express **17**, 2224–2234 (2009).

1. Introduction

Electromagnetic scattering from nanometer-scale objects has long been a topic of great interest and relevance to fields from astrophysics or meteorology to biophysics and material science [1–6]. During the last decade nano-optics has developed itself as a very active field within the nanotechnology community. Much of it has to do with plasmon (propagating) based subwavelength optics and applications [7], the synthesis of negative-index optical metamaterials [8–10] or the design of optical antennas [11–13].

Magnetic effects, a key ingredient of relevant microwave applications, cannot be easily exploited in the optical range (visible or infrared) due to intrinsic natural limitations of optical materials. The quest for magnetic plasmons and magnetic resonant structures at optical frequencies [14] has been mainly focused on metallic structures with the unavoidable problems of losses and saturation effects inherent to metals in the optical range. Moreover, their size is often required to be comparable to, or a fraction of, the operating wavelength in order to provide a non-negligible response, and their magnetic response is strongly affected and influenced by an intrinsic quadrupolar contribution, which introduces additional radiation losses and impurity of radiation and polarization [15].

As an alternative approach, there is a growing interest in the theoretical and experimental study of high-permittivity dielectric objects as constitutive elements of new metamaterials [16–25], negatively refractive photonic crystals [26, 27] and antennas based on dielectric resonators [28–30]. Large field resonant enhancements in the gap between two dielectric silicon microdisks have been predicted [31] to be comparable to those founded between metal nanoparticles. Interesting magnetodielectric properties are usually associated to low loss and large dielectric constants which, being accessible at microwave and terahertz frequencies, are still a challenging issue in the infrared (IR) and visible frequency ranges [32]. However, it has recently been shown [25] that silicon rod arrays could exhibit a true metamaterial left handed dispersion branch in the visible to mid-IR despite the moderate value of the refractive index ($m \sim 3.5$).

Motivated by these results, we have analyzed in detail the magnetodielectric properties of loss-less dielectric spheres made of moderate permittivity materials in the infrared regime. The scattering resonances of homogeneous spheres have been analyzed in the past [1–3]. Both electric and magnetic Mie resonances were studied for very large dielectric particles [33] and in smaller particles of very large refractive index, and at wavelengths being 100 times their radius [34]. We concentrate here on the relevance of the first magnetic dipolar resonance in non-absorbing dielectric nano-spheres (e.g. silicon spheres in the mid-IR). As we will see, submicron Silicon spheres (with radius $a \approx 200$nm) can present a strong magnetic resonance response at telecom and infrared frequencies, (namely, wavelengths $\lambda \approx 2ma \approx 1.5\mu$m). Moreover, in this frequency range, and based on standard Mie theory [1], we have found that *the scattering of these Si nanoparticles can be perfectly described by dipolar electric and magnetic fields; quadrupolar and higher order contributions being negligible*. Interestingly, the magnetic

#137123 - $15.00 USD Received 25 Oct 2010; revised 23 Dec 2010; accepted 15 Feb 2011; published 28 Feb 2011

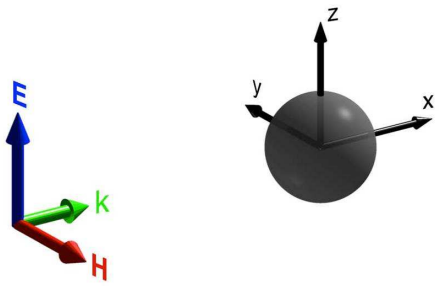

Fig. 1. Incident field vector.

resonance line remains well defined and resolved even for lower index materials, as Rutile-like TiO_2 with an average index $m \approx 2.45$ in the near-IR, even though in this latter case the electric dipole resonance line strongly overlaps with the magnetic dipole one, as well as with those of higher order multipoles. Subsequently, as an illustration we estimate the consequence of this magnetic resonance to build composites of Si spheres with a substantial effective magnetic permeability. Thus such particles constituting important candidates to be considered as metamaterial elements.

2. Extinction resonances of a dielectric sphere. The Mie theory revisited

Consider a non-absorbing dielectric sphere of radius a, index of refraction m_p and dielectric permittivity $\varepsilon_p = m_p^2$ in an otherwise uniform medium with real relative permittivity ε_h, permeability $\mu_h = 1$, and refractive index $m_h = \sqrt{\varepsilon_h}$. The magnetic permittivity of the sphere and the surrounding medium is assumed to be 1. Under plane wave illumination, and assuming linearly polarized light, the incident wave is described by

$$\mathbf{E} = E_0 \mathbf{u}_Z e^{ikX} e^{-i\omega t} \quad , \quad \mathbf{B} = B_0 \mathbf{u}_Y e^{ikX} e^{-i\omega t} \tag{1}$$

where $k = m_h \omega / c = m_h 2\pi/\lambda$, λ being the wavelength in vacuum and $B_0 = \mu_0 H_0 = -(m_h/c)E_0$ (see Fig. 1). The field scattered by the sphere can be decomposed into a multipole series, (the so-called Mie's expansion), characterized by the electric and magnetic Mie coefficients $\{a_n\}$ and $\{b_n\}$, respectively; (a_1 and b_1 being proportional to the electric and magnetic dipoles, a_2 and b_2 to the quadrupoles, and so on). We shall find useful to write the Mie coefficients in terms of the scattering phase-shifts α_n and β_n [1]

$$a_n = \frac{1}{2}\left(1 - e^{-2i\alpha_n}\right) = i \sin\alpha_n e^{-i\alpha_n} \tag{2}$$

$$b_n = \frac{1}{2}\left(1 - e^{-2i\beta_n}\right) = i \sin\beta_n e^{-i\beta_n} \tag{3}$$

where

$$\tan\alpha_n = \frac{m^2 j_n(y)\left[x j_n(x)\right]' - j_n(x)\left[y j_n(y)\right]'}{m^2 j_n(y)\left[x y_n(x)\right]' - y_n(x)\left[y j_n(y)\right]'}, \tag{4}$$

$$\tan\beta_n = \frac{j_n(y)\left[x j_n(x)\right]' - j_n(x)\left[y j_n(y)\right]'}{j_n(y)\left[x y_n(x)\right]' - y_n(x)\left[y j_n(y)\right]'}, \tag{5}$$

$m = m_p/m_h$ being the relative refractive index, $x = ka$ the size parameter and $y = mx$. $j_n(x)$ and $y_n(x)$ stands for the spherical Bessel and Neumann functions, respectively, and the primes

#137123 - $15.00 USD Received 25 Oct 2010; revised 23 Dec 2010; accepted 15 Feb 2011; published 28 Feb 2011

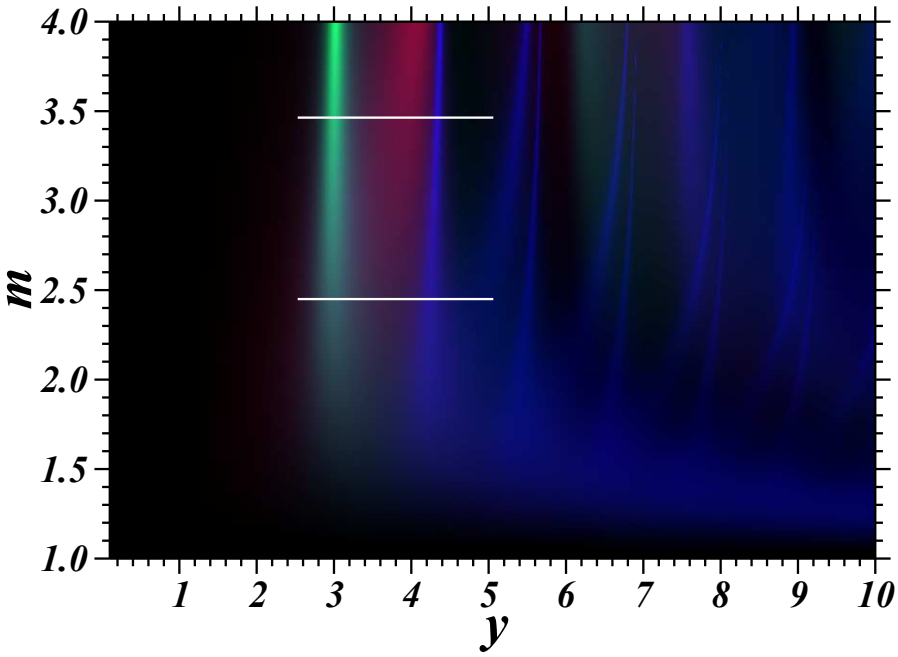

Fig. 2. Scattering cross section map of a non-absorbing Mie sphere as a function of the refractive index m and the y parameter, $y = mka = m(2\pi a/\lambda)$. Green areas correspond to parameter ranges where the magnetic dipole contribution dominates the total scattering cross section, while red areas represent regions where the electric dipole contribution is dominating. The remaining blue-saturated areas are dominated by higher order multipoles. Brightness in the color-map is proportional to the total cross section. White horizontal lines represent the y-range covered by figures 3 ($m = 3.5$) and 5 ($m = 2.45$).

indicate differentiation with respect to the argument. In absence of absorption, i.e. for real m, the phase angles α_n and β_n are real, then the extinction and scattering cross sections, σ_{ext} and σ_S, respectively, have the common value [1]

$$\sigma_S = \sigma_{\text{ext}} = \frac{2\pi}{k^2}\sum_{n=1}^{\infty}(2n+1)\left\{\sin^2\alpha_n + \sin^2\beta_n\right\} = \sum_{n=1}^{\infty}\left\{\sigma_{E,n} + \sigma_{M,n}\right\} \tag{6}$$

In the small particle limit ($x \ll 1$) and large particle permittivities ($m \gg 1$) the extinction cross section presents characteristic sharp resonance peaks. The values of $y = mx$ at which the angles α_n or β_n are $\pi/2, 3\pi/2, \ldots, etc$, define the resonance points. At each resonance, the extinction cross section is of the order of λ^2 and it is independent of either the particle size or the refractive index [1]

$$\sigma_S^{\text{res}} = \sigma_{\text{ext}}^{\text{res}}\big|_{\{x\ll 1\ ;\ m\gg 1\}} \approx \frac{2\pi}{k^2}(2n+1) \tag{7}$$

Asymptotically, the first resonance peak occurs at $y = \pi$ (i.e. $\lambda = m2a$) corresponding to the magnetic dipole term of coefficient b_1.

Interesting consequences and applications of well defined Mie resonance lines, associated to low loss and large dielectric constants, are accessible for different materials at microwave and terahertz frequencies. However, as m decreases there is an increasing overlap between the

#137123 - $15.00 USD Received 25 Oct 2010; revised 23 Dec 2010; accepted 15 Feb 2011; published 28 Feb 2011

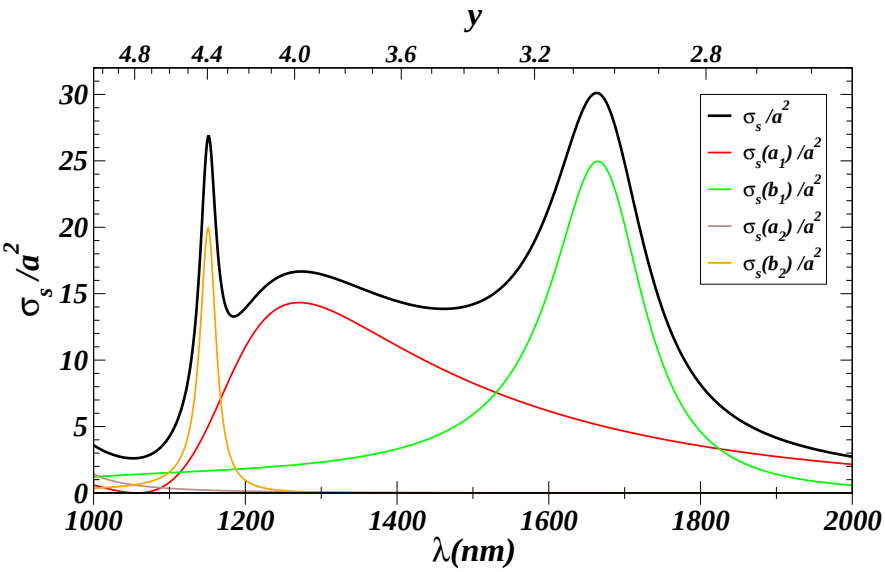

Fig. 3. Scattering cross-section σ_S versus the wavelength λ for a 230nm Si sphere (the refraction index $m = 3.5$ is constant and real in this wavelength range). The contribution of each term in the Mie expansion is also shown. The green line corresponds to the magnetic dipole contribution.

wavelength dependent cross-section peaks, and the sphere resonant response smears out. Since usually non-absorbing materials present low refractive index in the infrared (IR) and visible frequency ranges, Mie resonances of small particles in these regimes have not been considered in detail. However, the above analysis on the cross-section, carried out for Si nanoparticles in the IR, indicate that the aforementioned asymptotic behavior can be extended to a relative refractive index as low as $m \approx 3$.

In Fig. 2 we show the scattering cross section map of a non-absorbing Mie sphere as a function of the refractive index m and the y parameter, $y = m(2\pi a/\lambda)$. Brightness in the color-map is proportional to σ_{ext} while color code represents the contribution of electric and magnetic dipoles to the total cross section. The RGB (Red, Green, Blue) code is formed by taking $RGB = \sigma_{E,1}R + \sigma_{M,1}G + \sigma_{\text{res}}B$ with $\sigma_{\text{res}} \equiv \sqrt{\sigma_{\text{ext}}^2 - \sigma_{E,1}^2 - \sigma_{M,1}^2}$. The whole map is normalized to avoid over-saturation. Hence, green areas correspond to parameter ranges where the magnetic dipole contribution dominates the total scattering cross section, while red areas represent regions where the electric dipole contribution is dominating. The remaining blue-saturated areas are dominated by higher order multipoles.

In the micrometer wavelength regime, within the transparent region of silicon ($\lambda \gtrsim 1100$ nm), the index of refraction can well be approximated by a real constant $m_p \approx \sqrt{12} \sim 3.5$ (see for example [35]). The scattering (or extinction) cross section of a Si sphere of radius $a = 230nm$ in vacuum ($m_h = 1$) is plotted in Fig. 3. Although there is a partial overlap between the first dipolar peaks, the magnetic line of the first resonant peak (at $\lambda \approx 2ma$) is still very well resolved. Interestingly, for wavelengths larger than $\lambda \approx 1200$nm, the cross section is completely determined by the first b_1 and a_1 coefficients. In other words, in this regime Si particles can be treated as non-Rayleigh dipolar particles.

#137123 - $15.00 USD Received 25 Oct 2010; revised 23 Dec 2010; accepted 15 Feb 2011; published 28 Feb 2011

3. Magnetic and electric resonances of dipolar particles

Let us consider further in some detail the scattering properties of small dielectric particles ($x \ll 1$). In the $x \ll 1$ limit, the sphere is sufficiently small so that only the dipole scattered fields are excited. The induced dipole moments, proportional to to the external (polarizing) fields, **E** and **B**, are usually written in terms of the particle electric and magnetic polarizabilities α_E and α_M, respectively :

$$\mathbf{p} = \varepsilon_0 \varepsilon_h \alpha_E \mathbf{E} \quad , \quad \mathbf{m} = \frac{1}{\mu_0 \mu_h} \alpha_M \mathbf{B}; \tag{8}$$

where

$$\alpha_E = i \left(\frac{k^3}{6\pi} \right)^{-1} a_1 \quad , \quad \alpha_M = i \left(\frac{k^3}{6\pi} \right)^{-1} b_1. \tag{9}$$

By using the definition of the phase angles α_1 and β_1, [cf. Eqs. (2) - (5)], we can rewrite the polarizabilities as

$$\alpha_E = \frac{\alpha_E^{(0)}}{1 - i \frac{k^3}{6\pi} \alpha_E^{(0)}} \quad , \quad \alpha_M = \frac{\alpha_M^{(0)}}{1 - i \frac{k^3}{6\pi} \alpha_M^{(0)}}, \tag{10}$$

where

$$\alpha_E^{(0)} = -\frac{6\pi}{k^3} \tan \alpha_1 \quad , \quad \alpha_M^{(0)} = -\frac{6\pi}{k^3} \tan \beta_1. \tag{11}$$

In terms of these magnitudes, the extinction and scattering cross sections then read

$$\sigma_{\text{ext}} = k \text{Im} \{ \alpha_E + \alpha_M \} \tag{12}$$

$$\sigma_S = \frac{k^4}{6\pi} \left\{ |\alpha_E|^2 + |\alpha_M|^2 \right\} \tag{13}$$

Of course, in absence of absorption, $\alpha_E^{(0)}$ and $\alpha_M^{(0)}$ are real quantities and we recover the well known *optical theorem* result $\sigma_{\text{ext}} = \sigma_S$.

In particular, in the Rayleigh limit, when $y \equiv 2\pi ma/\lambda \ll 1$, $\alpha_E^{(0)}$ and $\alpha_M^{(0)}$ approach the quasi-static form,

$$\alpha_E^{(0)}\Big|_{y \ll 1} \approx 4\pi a^3 \frac{m^2 - 1}{m^2 + 2} \quad , \quad \alpha_M^{(0)}\Big|_{y \ll 1} \approx 4\pi a^3 (m^2 - 1) \frac{k^2 a^2}{30} \tag{14}$$

From Eq. (14), together with Eq. (10), we recover the well known expression for the polarizability of a Rayleigh particle including radiative corrections [6, 36, 37]. Notice that in this limit the magnetic polarizability is negligible. Very small particles always behave as point electric dipoles.

However, for particle sizes that are not extremely subwavelength, the quasi-static approach fails to describe the resonant behavior. *As y increases, (i.e. as λ decreases), there is a crossover from electric to magnetic behavior* as shown by Fig. 3 for a Si particle. The y values at which the quasi-static polarizability $\alpha_E^{(0)}$ ($\alpha_M^{(0)}$) diverges define the electric (magnetic) dipolar resonances. *Near the first b_1-resonance, the particle essentially behaves like a magnetic dipole* (cf. Fig. 2). If λ decreases further, a_1 peak dominates and the sphere becomes again an electric dipole. Notice however that, due to the overlap between the electric and magnetic responses,

#137123 - $15.00 USD Received 25 Oct 2010; revised 23 Dec 2010; accepted 15 Feb 2011; published 28 Feb 2011

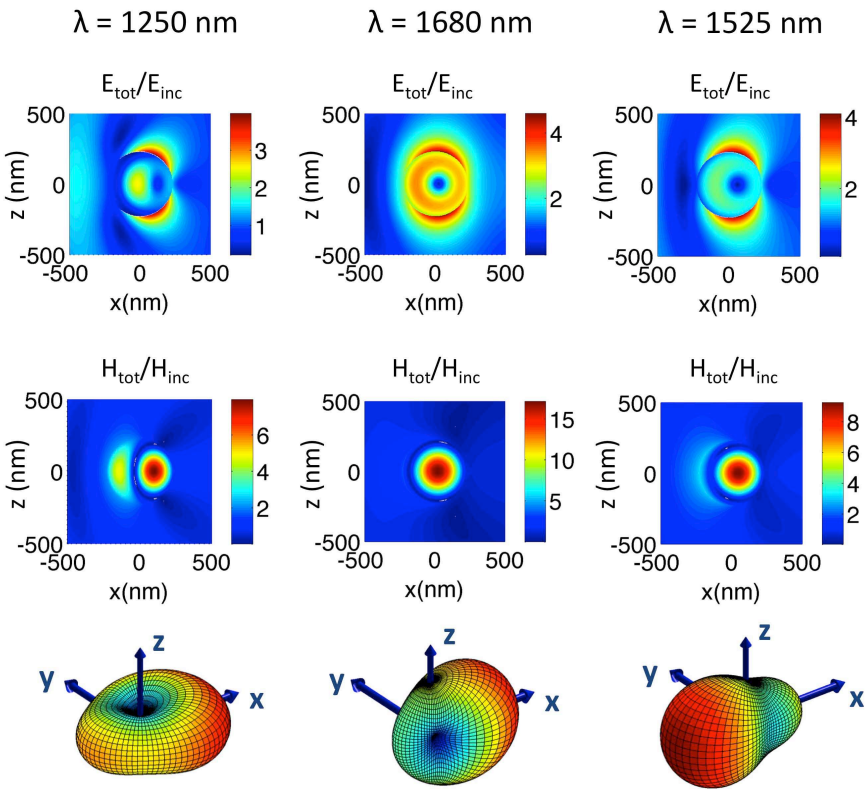

Fig. 4. Maps for the modulus of the total electric an magnetic vectors normalized to the incoming electric and magnetic field respectively ($E_{\rm tot}/E_{\rm inc}$ and $H_{\rm tot}/H_{\rm inc}$), for a Si nanoparticle of radius $a = 230$nm under plane wave illumination, (cf. Fig. 1). XZ planes crossing $y = 0$ are displayed. The left and central panels correspond to $\lambda = 1250$nm and $\lambda = 1680$nm of the electric and magnetic resonance peaks of Fig. 3, respectively. The right panel corresponds to the situation where the electric and magnetic resonances contribute equally to the scattering cross section ($\lambda = 1525$nm). The corresponding far field scattering radiation patterns for the three wavelengths are shown in the bottom row. The corresponding maps for YZ and XZ planes can be seen in the suplementary figure files (Media 1) and (Media 2), respectively.

#137123 - $15.00 USD Received 25 Oct 2010; revised 23 Dec 2010; accepted 15 Feb 2011; published 28 Feb 2011

the radiation field near the resonances does not correspond to a fully pure electric or a fully pure magnetic dipolar excitation. Yet, as seen in Fig.2 for the aforementioned Si sphere, the magnetic dipole contribution is, at its peak, about five times larger than the electric dipole one.

As a further example, we have plotted in Fig. 4 (left and central panels) both the near field amplitude maps in the XZ plane crossing the origin of coordinates ($y = 0$nm) and far field radiation patterns at the resonant peaks of a_1 and b_1, (cf. Fig. 3), numerically calculated from the full Mie solution (and not only from the dipolar approximation). The magnetic and electric nature of both resonances is clearly supported by these near and far field maps. For $\lambda = 1250$nm (left column), the electric field map shows the typical two-lobe distribution corresponding to an electric dipole oriented along the z axis. The far-field radiation pattern also presents the characteristic donut-like shape of a dipole oriented along the z-axis with a slight distortion originated by the weaker contribution of the magnetic dipole. For $\lambda = 1680$nm, the circular distribution of the electric field enhancement inside the sphere (mid-top panel) is a clear signature of the magnetic dipole oriented along the direction normal to the plane (y direction). The corresponding far field radiation pattern (mid-bottom panel) is also consistent. Cross sections of the near fields on the XZ and XY planes through the origin of coordinates are included as supplementary material (Media 1) and (Media 2).

It is interesting to notice that there is no restriction for the magnetic field enhancement of an electric dipole to be substantially large, mainly inside the particle (mid-left plot in Fig. 4). Equally, the electric field enhancement in and around the magnetic dipole can present large values (top-center plot in Fig. 4).

For a general wavelength, different modes contribute to the optical response of the system. We show this effect if the right panel of Fig. 4 for the special case where both the electric and magnetic resonances contribute equally to the scattering cross section of the Si nanosphere

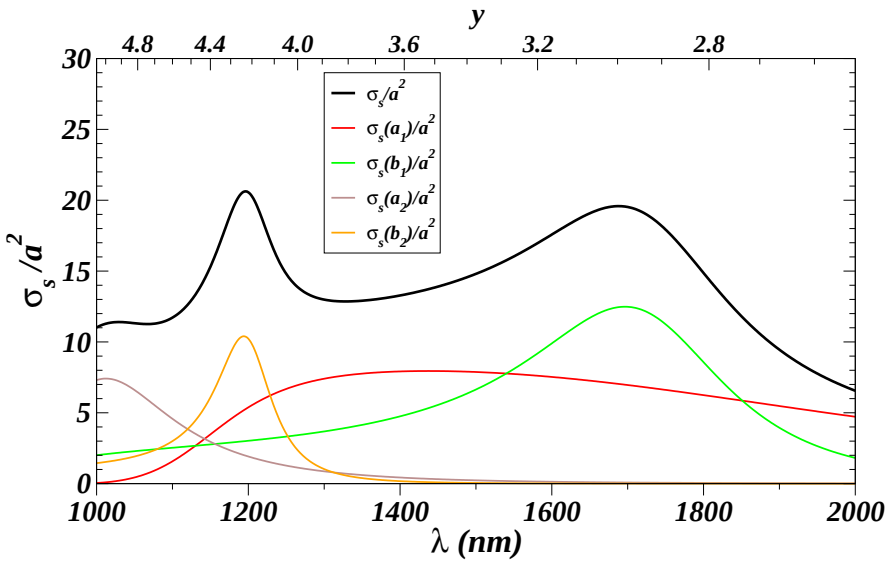

Fig. 5. Scattering cross-section σ_S versus the wavelength λ for a sphere of radius $a = 330nm$ (its relative refractive index is $m = \sqrt{6} \approx 2.45$, constant and real in this wavelength range). The contribution of each coefficient in the Mie expansion is also shown. The green peak at longer wavelengths corresponds to the magnetic dipole contribution.

#137123 - $15.00 USD Received 25 Oct 2010; revised 23 Dec 2010; accepted 15 Feb 2011; published 28 Feb 2011

($\lambda = 1525$nm, cf. Fig. 3). The near field patterns present mixed features of both electric and magnetic dipoles, and so does the far field with an interesting omnidirectional emission pattern as a result of the sum of both coherent contributions.

Silicon nanoparticles with radius of the order of 200-250nm are then fully characterized by electric and magnetic polarizabilities as given by Eqs. 10 in the mid and near-IR region. By tuning the appropriate resonance wavelength, Si particles exhibit a strong magnetic response, (only slightly perturbed by their electric dipole counterpart).

It should be remarked that if the relative refractive index is smaller, the overlap between the Mie resonance lines increases and, as it can be seen in Fig. 2, the first electric resonance smeared out for a refraction index lower than $m \lesssim 2.5$. Interestingly, the magnetic resonance line remains well defined and resolved even for lower index materials. As an example, in Fig. 5 we represent the scattering cross section of particle with $m = \sqrt{6} \approx 2.45$ which would correspond to the averaged refractive index of TiO_2 (rutile) in the near IR [35]. For comparison purposes, in order to cover the same y-range ($y = mka$) as in Fig. 3, we consider a larger sphere radius of $a = 330$nm. As seen in this figure, beyond 1400nm the scattering is still described by the sum of the electric and magnetic dipoles. While the magnetic resonance is still visible, the peak corresponding to the electric dipole, a_1, now disappears due to the strong overlap with the magnetic dipole one, as well as with those of higher order multipoles.

4. Composite of magnetodielectric Si particles

Among other possible applications, the strong dipolar magnetic resonance of Silicon submicron spheres endows them the potential of being exploited as elements of negative index materials, or in general of magnetodielectric metamaterials. Most of the current published work about magnetic resonances and dielectric metamaterials concentrate on dielectric spheres with very large relative permittivities (larger than ≈ 100) [17–21]. In the infrared spectral range, such high permittivities can be achieved by using materials with infrared polariton resonances which however present a relatively large absorption. Therefore, the non-absorbing dipolar response, both electric and magnetic of Si submicron spheres is of interest.

In practice, determining the effective constitutive parameters of such systems is a difficult problem, that can be solved only under (sometimes severe) approximations [38–40]. Lorentz-Lorenz theory is usually used to describe the effective response of composites made of an arbitrary arrangement of dipolar particles. Within this approach, if the composite is made of ρ spherical particles per unit volume, the effective permittivity ε_{eff} and permeability μ_{eff} are simply given by the Clausius-Mosotti equation [18, 21, 38]

$$\frac{\varepsilon_{\text{eff}} - 1}{\varepsilon_{\text{eff}} + 2} = f \frac{\alpha_E}{4\pi a^3} \quad ; \quad \frac{\mu_{\text{eff}} - 1}{\mu_{\text{eff}} + 2} = f \frac{\alpha_M}{4\pi a^3} \tag{15}$$

where $f = 4\pi a^3 \rho / 3$ is the filling fraction. This approach neglects positional correlations between particles and multiple scattering effects that could be relevant at relatively large filling fractions [40]. However, Eq. 15 would give a first guess on the relevance of the observed magnetic resonances in possible physical applications.

In order to obtain a preliminary estimation of the role that the Si spheres, addressed in Fig. 3, may have as building blocks of a continuum medium, or metamaterial, we plot in Fig. 6 the resulting values of the effective permittivity and permeability of an arbitrary arrangement of Si spheres for filling fractions $f = 0.25$ (a) and $f = 0.5$ (b) respectively. The free space wavelength at the magnetic resonance is about 4 times the diameter of the spheres. As it can be seen, the effective medium presents a remarkable dispersion in the effective permeability which is pivotal for most of the applications. For instance, one can play with these values of the effective constitutive parameters at chosen wavelengths to obtain real and imaginary parts

#137123 - $15.00 USD Received 25 Oct 2010; revised 23 Dec 2010; accepted 15 Feb 2011; published 28 Feb 2011

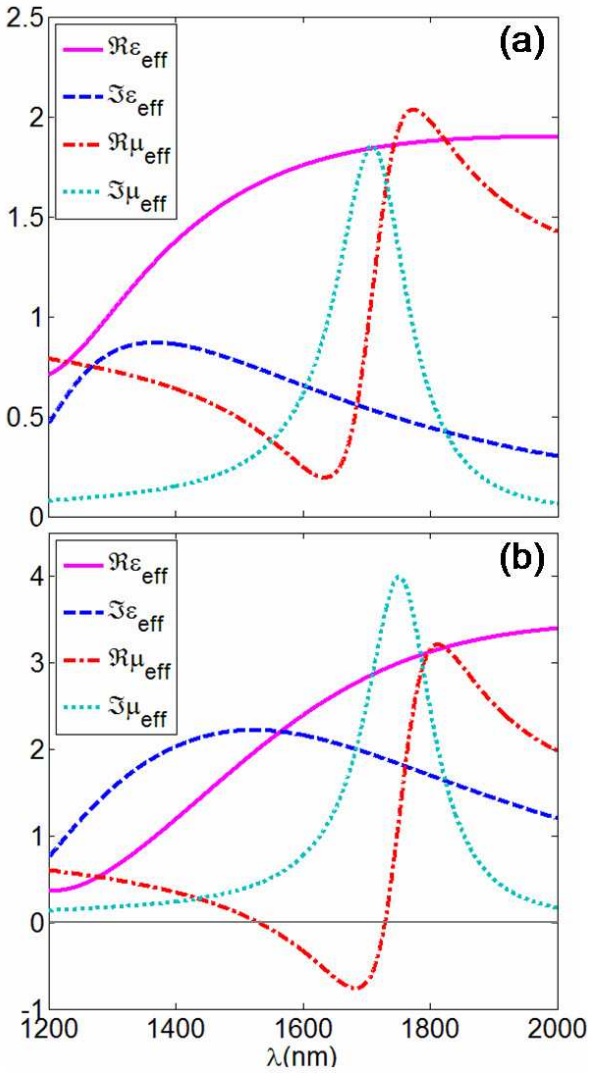

Fig. 6. Effective real and imaginary permittivities and permeabilities for an arbitrary arrangement of Si spheres in an otherwise homogeneous medium with $\varepsilon_h = \mu_h = 1$ for two different filling factors $f = 0.25$ (a) and $f = 0.5$ (b).

of the product $\varepsilon_{\text{eff}}\mu_{\text{eff}}$ that are adequately situated in the fourth quadrant of the complex plane to yield, in the selected branch, a convenient effective refractive index $m_{\text{eff}} = \sqrt{\varepsilon_{\text{eff}}\mu_{\text{eff}}}$, either with negative real part or not [19].

We should stress the absence of absorption (i.e. heating) in the system. Notice, however, that the effective constants are complex even in the case of a non-absorbing medium. Their imaginary parts being associated with the extinction of the propagating beam due to scattering (see, for example, Sec. 4.3 in Ref. [1] and [19, 41]).

#137123 - $15.00 USD Received 25 Oct 2010; revised 23 Dec 2010; accepted 15 Feb 2011; published 28 Feb 2011

5. Conclusion

We have analyzed the dipolar electric and magnetic response of lossless dielectric spheres made of both low and moderate permittivity materials. Based on the Mie expansion, we have derived general expressions for the electric and magnetic polarizabilities of dielectric spheres. We found that submicron Silicon particles present a strong magnetic resonant response in the mid-near infrared (wavelengths $\approx 1.2-2\mu$m). Interestingly, *the light scattered by these Si nanoparticles of appropriate size is perfectly described by dipolar electric and magnetic fields, being quadrupolar and higher order contributions negligible in this frequency range*. A preliminary estimation of the effective optical constants of an arbitrary arrangement of Si spheres suggest a remarkable dispersion in the effective permeability which is pivotal for most of the applications. These results can play an important role, not only in the field of metamaterials or optical antennas, but also in tailoring the light transport through complex dielectric media like photonic glasses [42, 43] with intriguing magnetic properties. Fabrication of new materials made of highly monodisperse subwavelength silicon spheres [44] may then lead to a new generation of magnetodielectric optical materials. At the magnetic or electric resonance wavelengths the extinction cross section is of the order of λ^2 reaching its maximum theoretical limit (independent of the particle size or refractive index) [1] (see also [30]). The large dipolar cross-section of magnetodielectric spheres near a magnetic resonance would also imply strong radiation pressure magnetic forces [37, 45, 46] leading to new concepts related to the optical forces on magnetic particles .

Acknowledgement

We appreciate interesting discussions with S. Albaladejo, B. Garcia-Camara, F. González, L. Inclán, F. Moreno, J.M. Saiz, I. Suárez and K. Vynck. This work has been supported by the EU NMP3-SL-2008-214107-Nanomagma and NoE Nanophotonics4Energy 248855, the Spanish MICINN Consolider *NanoLight* (CSD2007-00046), MAT2009-07841 GLUSFA and FIS2009-13430-C01 and C02, as well as by the Comunidad de Madrid Microseres-CM (S2009/TIC-1476) and PHAMA-CM (S2009/MAT-1756). F.S. and L.C. acknowledge financial support from the Swiss National Science Foundation, Projects No. 126772 and 117762. Work by R.G.-M. and L.S.F.-P. was supported by the MICINN "Juan de la Cierva" Fellowship.

#137123 - $15.00 USD Received 25 Oct 2010; revised 23 Dec 2010; accepted 15 Feb 2011; published 28 Feb 2011